Chapter 4 - Splice variants of Tissue Factor promote monocyte-endothelial interactions by triggering the expression of cell adhesion molecules via integrin ligation

R. Srinivasan, E. Ozhegov, Y.W. van den Berg, B.J. Aronow, R.S. Franco, M.B. Palascak, J.T. Fallon, W. Ruf, H.H. Versteeg and V.Y. Bogdanov

J Thromb Haemost. 2011 Oct;9(10):2087-96

Summary

Background: TF is highly expressed in cancerous and atherosclerotic lesions.Monocyte recruitment is a hallmark of disease progression in these pathological states. Objective: To examine the role of integrin signaling in TF-dependent recruitment of monocytes by endothelial cells. Methods: The expression of flTF and asTF in cervical cancer and atherosclerotic lesions was examined. Biologic effects of the exposure of primary microvascular endothelial cells (MVEC) to truncated flTF ectodomain (LZ-TF) and recombinant asTF were assessed. Results: flTF and asTF exhibited nearly identical expression patterns in cancer lesions and lipid-rich plaques. Tumor lesions, as well as stromal CD68+ monocytes/macrophages, expressed both TF forms. Primary MVEC rapidly adhered to asTF and LZ-TF, and this was completely blocked by anti-β1 integrin antibody. asTF- and LZ-TF-treatment of MVEC promoted adhesion of peripheral blood mononuclear cells (PBMCs) under orbital shear conditions and under laminar flow; asTF-elicited adhesion was more pronounced than that elicited by LZ-TF. Expression profiling and western blotting revealed a broad activation of cell adhesion molecules (CAMs) in MVEC following asTF treatment including E-selectin, ICAM-1 and VCAM-1. In transwell assays, asTF potentiated PMBC migration through MVEC monolayers by ~3-fold under MCP-1 gradient. Conclusions: TF splice variants ligate β1 integrins on MVEC, which induces the expression of CAMs in MVEC and leads to monocyte adhesion and transendothelial migration. asTF appears more potent than flTF in eliciting these effects. Our findings underscore the pathophysiologic significance of non-proteolytic, integrin-mediated signaling by the two naturally occurring TF variants in cancer and atherosclerosis.

Introduction

Alternatively spliced Tissue Factor (asTF) is a recently described, naturally occurring soluble form of Tissue Factor (TF) that lacks the transmembrane domain and exhibits lower pro-coagulant activity compared to decrypted full-length TF (flTF)[1]. Last year, we reported that human asTF possesses a biologic activity mechanistically distinct from that of flTF: asTF ligates integrins α6β1 and αvβ3 on endothelial cell (EC) surfaces, which triggers neovascularization in fVIIa- and/or PAR-2 independent manner[2]. asTF is more pro-angiogenic than flTF in aortic sprouting assays, and asTF protein levels in cervical cancer tissue were determined to be in 10-75 nM range, vastly exceeding those in systemic circulation, with asTF's biologic activity manifest at ~1 nM[2]. Plaque neovascularization is a major contributor to its destabilization: vasa vasorum as well as intraplaque vessels are microvascular in nature and the infiltration of the plaque by monocyte/macrophages is strongly associated with abnormal EC morphology[3]. Similarly to atheroslcerosis, tumor progression involves heavy infiltration of the tumor site by monocytes that differentiate

into M2-type macrophages secreting various tumor- and vessel-promoting cytokines[4]. Monocyte-endothelial interactions precede, and are required for monocyte transmigration[5,6]. Integrin ligation by asTF activates multiple kinases, including those comprising the PI3K/Akt pathway[2]. Engagement of PI3K/Akt signaling is known to activate NFκB[7] – a transcription factor involved in upregulation of leukocyte adhesion molecules that play a major role in atherogenesis. Of note, the levels of non-cellular TF are markedly increased in the aqueous humor of patients presenting with proliferative diabetic retinopathy – a condition in which leukocyte adhesion to microvascular EC (MVEC) is a major pathophysiological determinant[8,9].

While flTF and asTF proteins are detectable in organized mural thrombi, some atherosclerotic lesions, and various forms of cancer[1,10], it is not known whether these two naturally occurring TF variants may contribute to atherogenesis and/or tumorigenesis non-proteolytically by eliciting integrin-mediated biologic effects beyond the direct induction of neovascularization. In this study, we examined whether flTF and asTF act as agonists on MVEC – the endothelial subtype most relevant to monocyte egress from the systemic circulation.

Materials and Methods

Antibodies, chemicals and supplies- Please refer to Data S1 for a complete list of all antibodies, chemicals and cell culture supplies used in this study.

Tissue specimens, immunohistochemistry, and immunofluorescence studies- Use of de-identified banked specimens was approved by the Institutional Review Board of Leiden University Medical Center (Leiden, The Netherlands), Mount Sinai School of Medicine (New York, USA), and Charite Clinic (Berlin, Germany). Serial sections of formalin-fixed, paraffin-embedded specimens were deparaffinized, analyzed using standard immunohistochemical techniques as described[1,11], and images were captured using BX51 microscope and DP72 camera (Olympus). For immunofluorescence studies, serial sections were deparaffinized and double-stained for CD68/asTF, CD34/asTF, CD68/flTF, and CD34/flTF as follows. Sections were incubated for 3 hrs with anti-CD68/anti-CD34 mouse monoclonal antibody and the previously described and characterized[1,12] asTF/flTF-specific custom polyclonal rabbit antibodies, washed, and incubated for 30 min with goat anti-rabbit Alexa Fluor 488 and goat anti-mouse Alexa Fluor 594 antibodies (Invitrogen). Sections were mounted using Vectashield with DAPI (Vector Laboratories), and images captured using Nikon Photostat-FXA fluorescent microscope and Spot 2 camera (Diagnostic Instruments, Inc).

Cell culture- Primary human cardiac MVEC were purchased from Lonza. Cells were grown in EBM medium supplemented with antibiotics (Lonza). Primary human retinal MVEC were purchased from Cell Systems and maintained in MCDB-131 medium (Cell Systems). For experiments, MVEC between passages 3 and 6 were used. THP-1 cells (ATCC) were maintained in complete RPMI medium as previously described[12].

RT-PCR- Please refer to the Data S1 for the list of primers employed for RT-PCR

Flow cytometry-MVEC were grown to confluence and detached using 2 mM EDTA in PBS. Cells were centrifuged, washed in PBS, blocked in 1% BSA, incubated with anti-β1/β3 antibodies for 30 min on ice, washed in PBS, and incubated with anti-mouse goat-IgG (Alexa-488) for 30 min on ice. Cells were then washed with PBS, and flow cytometry was performed using Epics XL (Beckman Coulter) with 525 band pass filter.

Human TF proteins-Recombinant human asTF mature peptide with an N-terminal His-tag followed by the enterokinase cleavage site (DDDDK) was produced in E. Coli and purified as previously described[2]; asTF purity and identity were confirmed by Coomassie staining and western blotting, respectively (not shown); asTF's biologic activity was preserved following the cleavage of the His-tag and removal of enterokinase (Data S1). Recombinant human flTF extracellular domain with the GCN4 leucine zipper domain at the C-terminus (LZ-TF) was previously described[13].

MVEC adhesion assay- asTF and LZ-TF (100 ng/well) were used to coat 96-well tissue culture plates; 10% BSA (100 ul/well) served as control. MVEC were trypsinized, neutralized using serum-containing media, washed, added to 96-well plates at 20,000 cells/well and left to adhere under 5% CO2 at 37ºC for 2 hrs. Following the incubation, non-adherent cells were removed by washing the wells twice with PBS. The adherent cells were fixed in methanol, stained with crystal violet (Sigma), and counted at 10X using phase-contrast inverted microscope (Olympus) in three random fields excluding the edges.

Monocyte-MVEC interaction assays- Orbital shear assay: MVEC were grown to confluence in 96-well plates, after which LZ-TF/asTF (final concentration 50 nM) was added to the wells for 4 hrs; equal volumes of 50% glycerol in PBS served as the vehicle control. Functional blocking studies of LZ-TF/asTF were carried out using 6B4 antibody (100 µg/ml) that hinders TF association with integrins[2]. THP-1 cells were labeled with 1 uM Calcein-AM for 30 min, washed in serum-free media, and placed in 96-well plates added at 1.5 x 105 cells/well on orbital shaker set at 90 rpm in a humidified incubator at 37oC and 5% CO2 for 1 hr. Following the incubation, plates were washed with PBS to remove non-adherent THP-1 cells and lysed with 0.1% Triton-X in PBS for 15 min. Fluorescence was measured at

Ex-485 and Em-535 in Omega Fluorimeter (BMG Labtech). Static adhesion assays were performed as per the orbital shear assay, with the exception of the MVEC-THP-1 incubation step that was carried out under static conditions.

Parallel plate flow assay- MVEC were seeded in 35-mm tissue culture dishes and allowed to reach confluence over the course of 3-4 days, following which recombinant asTF or LZ-TF (final concentration – 50 nM) was added to the medium for 4 hrs; equal volumes of 50% glycerol in PBS served as the vehicle control. Cells were washed with serum-free media and assembled onto the flow chamber (Glycotech); subsequently, THP-1 cells were perfused through the chamber at 0.5 X 106 cells/ml in RPMI-1640 media at 37ºC using a syringe infusion pump (Harvard Apparatus) under phase-contrast inverted microscope (Olympus, PA); the shear rate was set to 0.5 dynes /cm2 (0.05 Pa). Video recordings were made using Moticam camera (Motic) and adherent cells were counted; each THP-1 cell that adhered to the endothelium for at least 1 sec was deemed a firm adhesion / cell arrest event.

Microarray analysis- MVEC were treated for 4 h with recombinant asTF or LZ-TF added to the medium (final concentration, 50 nM); equal volumes of 50% glycerol in PBS served as the vehicle control. Total RNA was isolated using RNAeasy kit (Qiagen, Valencia, CA, USA) R&D Systems (Minneapolis, MN, USA), reverse transcribed, amplified, fragmented, and labeled for microarray analysis using the Nugen WT-Ovation FFPE V2 kit, Exon Module and Encore biotin module (Nugen), respectively, according to the manufacturer's instructions. Affymetrix Human Gene 1.ST microarray chips were used to assess the gene expression profile (Microarray Core Facility, Cincinnati Children's Hospital and Medical Center). Transcripts that were differentially expressed as a result of either LZ-TF or asTF treatment were identified based on filtering for probesets with Robust Multichip Average-normalized raw expression of greater than 6.0 in either of the three pairs of replicates, that differed between treated and untreated MVEC by at least 1.5-fold with $P<0.05$ using a Welch t-test. Using this approach, we identified 223 genes that were upregulated in both MVEC subtypes by asTF, and 63 by LZ-TF.

Western blotting- Please refer to Data S1 for the list of reagents used for Western blotting.

Transendothelial migration assay- MVEC were grown to confluence on 0.3 um cell culture inserts (Millipore) and treated with asTF (final concentration – 50 nM) for 4 hrs, following which the receiver plate was replaced with the media containing 50 µg/L recombinant MCP-1 (R&D Systems). 3 X 10^5 THP-1 cells / insert were added to the upper chamber for 1 hr, following which the non-adherent cells were removed, fresh medium was added, and the adherent THP-1 cells were left to migrate overnight in 5% CO2 at 37ºC. The following

day, THP-1 cells at the luminal side of the insert were carefully removed by a cotton swab, the insert was excised, fixed in methanol, and the migrated THP-1 cells on the abluminal side of the insert were stained with DAPI. Cells were counted at three different randomly selected locations on the membrane, excluding the edge.

Statistical analysis- The comparisons of means were performed using Student t-test. Two-sided p-values less than 0.05 were considered statistically significant.

Results

Co-localization of flTF and asTF in cervical cancer tissue and atherosclerotic plaques- While it is known that asTF protein is present in cervical cancer tissue at concentrations in the 10–75 nM range, the cellular sources of asTF and/or the concomitance of asTF's expression with that of flTF has not been evaluated[2]; likewise, asTF was observed in organized spontaneous thrombi and atherosclerotic material, yet its cellular sources and/or co-localization with flTF were not examined in detail[1,10]. We analyzed themexpression of flTF and asTF in sets of formalin-fixed, paraffinembedded specimens of cervical adenocarcinoma (50% + relative tumor mass, n = 10) and lipid-rich aortic plaques (n = 10). In cervical adenocarcinoma, flTF and asTF expression patterns appeared nearly identical, with extensive colocalization in most, yet not all, tumor lesions (Fig. 1A); in aortic plaques, flTF expression appeared more pronounced than that of asTF and again, overlapping patterns were observed for flTF and asTF (Fig. 1B). Aside from tumor lesions, stromal cells were also positive for flTF and asTF (Fig. 1A,B); we performed immunofluorescence studies using anti-CD68 antibodies and anti-fl/asTF-specific antibodies (Fig. 2): asTF and flTF were found in abundance in $CD68^+$ cells – monocytes/macrophages (Fig 3, S1). asTF staining in the extracellular space was clearly evident (Fig. 3A,B), in line with the fact that asTF can be secreted[14,15]. $CD68^+$ cells were also found to express flTF and asTF in aortic plaques (Fig. 3B).

flTF and asTF ligate β1 integrins on MVEC surfaces- The αV integrin chain is expressed in human MVEC[16], yet it is not known whether MVEC express the b1 and b3 integrin chains that interact with flTF as well as asTF[2]. β1 and β3 mRNA species were detected in cardiac and retinalMVEC; β3 mRNA expression appeared lower than that of β1 mRNA in both MVEC subtypes (not shown). Cell-surface expression of β1 and β3 integrins was analyzed by flow cytometry and again, β3 integrin levels were remarkably lower than those of β1 in both MVEC subtypes (Fig. 4A). We then performed cell adhesion assays to determine whether MVEC can bind TF isoforms. For flTF studies, we employed LZ-TF, the extracellular domain of human flTF able to form non-covalent homodimers and previously shown to

effectively bind to integrins[13]. An approximately 20-fold increase in adhesion of cardiac and retinal MVEC was observed as early as 30 min after MVEC were placed in LZ-TF/asTF-coated wells ($P < 0.001$, Fig. 4B). To determine the relative contributionof β1 and β3 integrins to LZ-TF/asTF binding by MVEC, we preincubated the cells with inhibitory antibodies to each specific integrin chain. b1 blockade effectively abolished MVEC adhesion to LZ-TF and asTF ($P < 0.05$), whereas β3 blockade had no effect in either MVEC subtype (Fig. 4B). We note that the markedly lower levels of β3 integrins were proposed to be a characteristic of microvascular, as opposed to macrovascular, endothelial cells[16].

flTF and asTF promote MVEC-monocyte interactions- The ligation of β1 integrins on MVEC surfaces by both forms of TF prompted us to investigate whether flTF and asTF promote EC-monocyte interactions – a crucial hallmark in the progression of cancer and atherosclerosis. We employed two assays designed to recapitulate the conditions within the (micro)circulatory tree in distinct pathological settings, i.e. the static assay simulating near-stasis conditions in the post-capillary venules, and the orbital shear assay simulating the conditions in recirculation zones of partially occluded vessels where cyclic shear stress predominates. LZ-TF and asTFtreatedMVEC revealed increased interaction with PBMC: inthe orbital shear assay, a ~130% increase in PBMC adhesionwas observed in response to asTF and ~65% in response toLZ-TF ($P < 0.01$, Fig. 4C); of note, asTF potentiated PBMC adhesion to MVEC at 0.1 nM in this assay (Fig. 4D). The monoclonal antibody 6B4 that binds to the integrin-binding domain of TF^2 potently inhibited the effects of LZ-TF as well as asTF in enhancing the monocyte-MVEC interactions (Fig. S2). To rule out the possibility that the effects of asTF were elicited by traces of endotoxin in protein preparations, we performed a series of control experiments: addition of LPS inhibitor polymyxin B to MVEC cultures as well as asTF preparations and/or incubation with non-charged agarose beads did not affect the experimental outcome, whereas the depletion of asTF with Ni-charged beads and heat denaturation eliminated the observed effects, confirming that the observed phenomena are asTF specific (Fig S3 and data not shown). In the laminar flow assay, asTF again elicited amore pronounced effect compared with LZ-TF: a ~6-foldincrease in PBMC adhesion was observed for asTF-stimulated MVEC ($P < 0.001$) compared with a ~3-fold increase for LZTF-stimulated MVEC ($P < 0.05$, Fig. 4E). To identify the intracellular pathways employed by asTF to potentiate monocyteadhesion to MVEC, we performed orbital shear assays inwhich MVEC were pretreated with a panel of integrin-linked kinase inhibitors. asTF-triggered enhancement of the interactions between cardiac MVEC and monocytes was completely suppressed by PI3K/Akt inhibitor LY294002 and by NFκB inhibitor BMS345541, whereas inhibition of p38 MAPK, p42/p44 MAPK, FAK and/or ROCK had no effect (Fig. 4F); theresults obtained with retinal MVEC were analogous (not shown).

Ligation of β1 integrins by asTF elicits global changes in gene expression in MVEC- Of the two forms of human TF, the minimally coagulant asTF is a more potent inducer of integrin-mediated angiogenesis[2]. Multiple kinases are engaged in response to asTF ligation inmurine and human macrovascular cells[2], the combined effectof which results in a remarkable potentiation of monocyteadhesion (Fig. 4C–F). We evaluated the nature of the changesin global gene expression elicited by LZ-TF and asTF inMVEC and the extent to which these changes were independentof the MVEC subtype, using microarrays. The concordance among the genes whose expression was upregulated by LZ-TF and asTF in cardiac or retinal MVEC was high, yet the nature of the response to asTF and LZ-TF at the ≥1.5-fold cutoffwas remarkably different (Fig. 5A). Of the 813 probesets that exhibited a significant up- or downregulation elicited by asTF in either MVEC subtype (FDR < 0.05, Benjamini Hochberg), 332 probesets corresponding to 223 genes were upregulated ≥1.5-fold by asTF in both MVEC subtypes. The major categories of their function were identified using ToppGene and are listed in Table 1; they include a broad range of defense response, cytokine signaling and NFκB-drivenprograms/pathways associated with cell adhesion, cell migration, innate immunity and wound healing. Specifically, transcription of several classes of genes was upregulated by asTF inboth MVEC subtypes: (i) growth factor genes such as VEGF-A and FGF, (ii) genes encoding cell adhesion molecules(CAMs) E-selectin, VCAM-1, and cytokines including CCL2,CCL20, CCL5, CXCL3 and IL-1A, the molecules implicated in attracting peripheral blood monocytes[17]; (iii) genesgoverning apoptosis, of which ~70% were anti-apoptotic (e.g. NFKB1 and SERPINB2), as well as genes promoting EC migration and proliferation (e.g. RELB; (iv) genes encodingvarious transcription factors governing cytokine expression (e.g. CEBPD, KLF-7 and NRIP1); and (v) genes involved in metabolic processes (e.g. APOL3, PISD, COX6A1), iron transport (e.g. SLC7A11, SLC39A6, SLC7A5), and structural proteins (e.g. FNDC3B, COLA6, PSEN1) (Fig. 5A, Table S1and data not shown). In contrast to asTF, LZ-TF potentiated ≥1.5-fold upregulation of 63 genes in MVEC, most notable of which were seven genes encoding snoRNA (Fig. 5A). E-selectin,VCAM-1 and ICAM-1 were markedly upregulated on mRNA and protein levels in asTF-treated cardiac and retinalMVEC (Fig. 5B,C). The upregulation of these three CAMs was blocked by PI3K and NFκB inhibitors as well as anti-β1 antibody, which had a particularly striking effect on the levels of E-selectin (Fig. 5D); the effect of anti-β3 antibody did not differ from that of isotype control IgG (not shown). Although we previously demonstrated that asTF-triggered, integrin-mediated signaling elicits angiogenesis[2], this is the first report on the ability of the (as)TF/integrin axis to significantly upregulate the expression of CAMs in human EC.

Transendothelial migration of monocytes adhered to MVEC in response to asTF stimulation- Monocyte egress from the lumen is highly significant in themacrovascular as

well as microvascular contexts: monocytes act as a rich source of TF leading to a procoagulant environment in the arterial wall. We sought to examine whether asTF is able to promote monocyte transmigration inthe presence of CCL2/MCP-1, whose transcription was induced by asTF. In a transwell assay, the migration of PBMCs as well as THP-1 cells across asTF-stimulated MVEC monolayers was enhanced >3-fold when MCP-1 was present on the abluminal side of the insert; this effect was fully inhibitedby anti-β1 antibody whereas the effect of anti- β3 antibody did not differ from that of isotype control IgG ($P < 0.001$, Fig. 6,S4 and data not shown).

Discussion

This is the first report on the ability of the TF-integrin axis to upregulate CAMs in human EC as a result of integrin ligation, leading to the increased EC-monocyte interactions. Monocyte recruitment contributes to the progression of atherosclerosis, diabetic retinopathy, and many forms of neoplasia[4,5,9]. We here demonstrate that flTF and asTF co-localize with $CD68^+$ cells in cervical cancer and aortic plaque specimens; thus, tumor cells as well as stromal cells are likely to contribute to the high concentrations of asTF protein found in cervicalcancer[2]. Atherosclerotic plaques display a uniform pattern of flTF/asTF co-localization with $CD68^+$ monocytes/macrophages, suggesting a possible feedback loop whereby the monocytes recruited to the developing plaque synthesize TF variants that further augment monocyte/macrophage accumulation by promoting their adhesion to MVEC via ligation of β1 integrins. We note that flTF was recently reported to upregulate the expression of mRNA encoding E-selectin and various chemokines in human macrovascular cells (HUVEC)[18]. The remarkable potency of asTF under laminar flow, and asTF-elicited upregulation of CXC and CC chemokines, support the notion that asTF, alongside flTF, may play a major role in atherogenesis[14]. Of note, it was reported that a systemic 50% reduction in total TF and selective elimination of total TF expression in hematopoietic cells does not affect atherosclerotic phenotype in the genetically modified mouse models[19]; thus, asTF effects are likely to be mostly relevant to solid cancer tissues where asTF protein levels are relatively high[2].However, many differences exist between humans and mice, particularly with regard to monocyte subpopulations and their relative importance in disease progression[20,21]; thus, new mouse models featuring splice isoform-specific TF phenotypes are needed to assess the significance and relative contributions of the TF splice variants to the pathobiology of cancer and/or atherosclerosis. We here demonstrate that compared withrecombinant truncated flTF (LZ-TF), asTF is a more potent inducer of the three essential CAMs (ICAM-1, VCAM-1 and E-selectin) required for the firm adhesion of leukocytes to the endothelium[21]. We found a highly significant increase inmonocyte adhesion to LZ-TF/asTF-exposed MVEC in two distinct assays

simulating various flow conditions, performed inthe defined medium free of FVII(a). Orbital shear and laminar flow assays revealed that while both forms of TF increase monocyte adhesion to MVEC, asTF is much more potent when freshly isolated blood PBMC are employed, and it markedly potentiates monocyte transmigration across MVEC monolayers in the presence of a chemokine gradient. While the PI3K/Akt-NFκB pathway appears to play a critical role in TF-triggered upregulation of CAMs in human MVEC, it cannot be excluded that flTF/asTF might also recruit other integrin binding proteins, such as uPAR, to differentially modulate signaling in specific EC subtypes[22].

Our data indicate that cells of monocytic origin appear to be the major source of flTF/asTF within the plaque, which is in agreement with the earlier findings that CD14+ cells are the major source of flTF and asTF in systemic circulation[1]. In an elegant study by Borisoff et al., early and late atherosclerotic lesions were found to be the sites of active local synthesis of several coagulation proteins, including TF,with the early lesions exhibiting a more procoagulant phenotype[23]. As the monocytes recruited to the plaque greatly contribute to its instability, characterized by the graduate change of the plaque phenotype from proliferative to inflammatory/pro-angiogenic in the course of atherosclerotic progression[24], it is reasonable to propose that the “TF isoform profile” of the intraplaque monocytes/macrophages may also evolve; the biosynthesis of asTF mRNA is largely dependent on the activity of the splicing regulator (SR) proteins ASF/SF2, SRp55, SRp40, SC35 and SRp75, whose functional interplay in the course of TF pre-mRNA processingis controlled by several kinases sensitive to the extracellular environment[12,25,26].While it has now been established that TFis locally synthesized within the plaque during its progression from early-procoagulant to advanced-inflammatory/pro-angiogenic[23], it is yet to be examined whether a decrease in flTF biosynthesis with a concomitant increase in asTF biosynthesis may contribute to the change of the plaque phenotype. Monocyte transmigration across the EC monolayer is a hallmark event in atherogenesis[5,6,24]; we stress that leukocyte infiltration of the plaque occurs chiefly through microvascular EC[3]. We propose that monocyte/foam cell-derived flTF and asTF may stimulate MVEC to produce adhesion molecules and chemokines to recruit additional monocytes, which can in turnsupport flTF/asTF accumulation; the expression of both formsof TF is markedly increased when human monocytes come intocontact with fibronectin[27].

In sum, our results expand the scope of the TF system’s non-proteolytic,integrin-mediated effects, underscoring the significance of high flTF/asTF expression for tumor progression and, possibly, atherogenesis. asTF, while being minimally coagulant, is likely to promote the recruitment of (i) potentially pro-angiogenic monocytes to cancer lesions and (ii) potentially procoagulant monocytes to the developing plaque; thus, asTF may represent a

novel therapeutic target: the impairment of asTF's function may significantly slow tumor growth as well as the progression of vascular lesions, while having only minimal effect on the maintenance of normal hemostasis.

Author contribution

R. Srinivasan*, E. Ozhegov* and M.B. Palascak* performed experiments, analyzed data, and wrote the paper; Y.W. van den Berg†, B.J. Aronow‡, R.S. Franco*, J.T. Fallon§, W. Ruf¶, and H.H. Versteeg† analyzed data, provided key reagents, and contributed to writing the paper; V.Y. Bogdanov* conceived the research, analyzed data, and wrote the paper.

Acknowledgements

This study was partially supported by NIH grant HL094891 to V.Y.B. The authors thank Prof. Dr. Ursula Rauch (Charite-Berlin) for providing the specimens of lipid-rich aortic plaques.

References

1. Bogdanov VY, Balasubramanian V, Hathcock J, Vele O, Lieb M, Nemerson Y. Alternatively spliced human tissue factor: a circulating, soluble, thrombogenic protein. Nat Med 2003;9:458-462.
2. van den Berg, YW, van den Hengel LG, Myers HR, Ayachi O, Jordanova K, Ruf W, Spek CA, Reitsma PH, Bogdanov VY, Versteeg HH. Alternatively spliced Tissue Factor induces angiogenesis through integrin ligation. Proc Natl Acad Sci USA 2009;106:19497-19502.
3. Sluimer JC, Kolodgie FD, Bijnens AP, Maxfield K, Pacheco E, Kutys B, Duimel H, Frederik PM, van Hinsbergh VW, Virmani R, Daemen MJ. Thin-walled microvessels in human coronary atherosclerotic plaques show incomplete endothelial junctions relevance of compromised structural integrity for intraplaque microvascular leakage. J Am Coll Cardiol 2009;53:1517-1527.
4. S.B. Coffelt, R. Hughes and C.E. Lewis: Tumor-associated macrophages: effectors of angiogenesis and tumor progression. Biochim Biophys Acta 2009;1796, 11-18
5. Mestas J, Ley K. Monocyte-endothelial cell interactions in the development of atherosclerosis. Trends Cardiovasc Med 2008;18:228-232.
6. Cybulsky MI, Gimbrone Jr MA. Endothelial expression of a mononuclear leukocyte adhesion molecule during atherogenesis. Science 1991;251:788-791.
7. Ozes ON, Mayo LD, Gustin JA, Pfeffer SR, Pfeffer LM, Donner DB. NFkappaB activation by tumour necrosis factor requires the Akt serine-threonine kinase. Nature 1999;401:82-85.
8. Sakamoto T, Ito S, Yoshikawa H, Hata Y, Ishibashi T, Sueishi K, Inomata H. Tissue factor increases in the aqueous humor of proliferative diabetic retinopathy. Graefes Arch Clin Exp Ophthalmol 2001;239:865–871.
9. Schroder S, Palinski W, Schmid-Schonbein GW. Activated monocytes and granulocytes, capillary nonperfusion, and neovascularization in diabetic retinopathy. Am J Pathol 1991;139:81–100.
10. van den Berg YW, Versteeg HH. Alternatively spliced tissue factor. A crippled protein in coagulation or a key player in non-haemostatic processes? Hämostaseologie 2010;30:144-149.

11. Sovershaev MA, Egorina EM, Bogdanov VY, Seredkina N, Fallon JT, Valkov AY, Østerud B, Hansen JB. Bone morphogenetic protein -7 increases thrombogenicity of lipid-rich atherosclerotic plaques via activation of tissue factor. Thromb Res 2010;126:306-310.
12. Tardos JG, Eisenreich A, Deikus G, Bechhofer DH, Chandradas S, Zafar U, Rauch U, Bogdanov VY. SR proteins ASF/SF2 and SRp55 participate in tissue factor biosynthesis in human monocytic cells. J Thromb Haemost 2008;6:877-884.
13. Dorfleutner A, Hintermann E, Tarui T, Takada Y, Ruf W. Cross-talk of integrin alpha3beta1 and tissue factor in cell migration. Mol Biol Cell 2004; 15: 4416–25. Cell 2004; 15: 4416–25.
14. Szotowski B, Antoniak S, Poller W, Schultheiss HP, Rauch U. Procoagulant soluble tissue factor is released from endothelial cells in response to inflammatory cytokines. Circ Res 2005;96:1233-1239.
15. Hobbs JE, Zakarija A, Cundiff DL, Doll JA, Hymen E, Cornwell M, Crawford SE, Liu N, Signaevsky M, Soff GA. Alternatively spliced human tissue factor promotes tumor growth and angiogenesis in a pancreatic cancer tumor model. Thromb Res 2007;120 Suppl 2:S13-21.
16. Wilson SH, Ljubimov AV, Morla AO, Caballero S, Shaw LC, Spoerri PE, Tarnuzzer RW, Grant MB. Fibronectin fragments promote human retinal endothelial cell adhesion and proliferation and ERK activation through alpha5beta1 integrin and PI3-kinase. Invest Ophthalmol Vis Sci 2003;44:1704-1715.
17. Tedgui A, Mallat Z. Cytokines in atherosclerosis: pathogenic and regulatory pathways. Physiol Rev 2006;86:515-581.
18. Grosser M, Magdolen V, Baretton G, Luther T, Albrecht S. Gene expression analysis of HUVEC in response to TF-binding. Thromb Res 2010; 127: 259–63.
19. Tilley RE, Pedersen B, Pawlinski R, Sato Y, Erlich JH, Shen Y, Day S, Huang Y, Eitzman DT, Boisvert WA, Curtiss LK, Fay WP, Mackman N. Atherosclerosis in mice is not affected by a reduction in tissue factor expression. Arterioscler Thromb Vasc Biol 2006; 26: 555–62.
20. Wilson HM. Macrophages heterogeneity in atherosclerosis – implications for therapy. J Cell Mol Med 2010; 14: 2055–65.
21. Woollard KJ, Geissmann F. Monocytes in atherosclerosis: subsets and functions. Nat Rev Cardiol 2010; 7: 77–86.
22. Smith HW, Marshall CJ. Regulation of cell signalling by uPAR. Nat Rev Mol Cell Biol 2010; 11: 23–36.
23. Borissoff JI, Heeneman S, Kilinc¸ E, Kassák P, van Oerle R, Winckers K, Govers-Riemslag JW, Hamulyák K, Hackeng TM, Daemen MJ, Ten Cate H, Spronk HM. Early atherosclerosis exhibits an enhanced procoagulant state. Circulation 2010; 122: 821–30.
24. Weber C, Zernecke A, Libby P. The multifaceted contributions of leukocyte subsets to atherosclerosis: lessons from mouse models. Nat Rev Immunol 2008; 8: 802–15.
25. Chandradas S,Deikus G, Tardos JG,Bogdanov VY. Antagonistic roles of four SR proteins in the biosynthesis of alternatively spliced tissue factor transcripts in monocytic cells. J Leukoc Biol 2010; 87: 147–52.
26. Eisenreich A, Bogdanov VY, Zakrzewicz A, Pries A, Antoniak S, Poller W, Schultheiss HP, Rauch U. Cdc2-like kinases and DNA topoisomerase I regulate alternative splicing of tissue factor in human endothelial cells. Circ Res 2009; 104: 589–99.
27. Bajaj MS, Ghosh M, Bajaj SP. Fibronectin-adherent monocytes express tissue factor and tissue factor pathway inhibitor whereas endotoxin-stimulated monocytes primarily express tissue factor: physiologic and pathologic implications. J Thromb Haemost 2007; 5:1493–9.

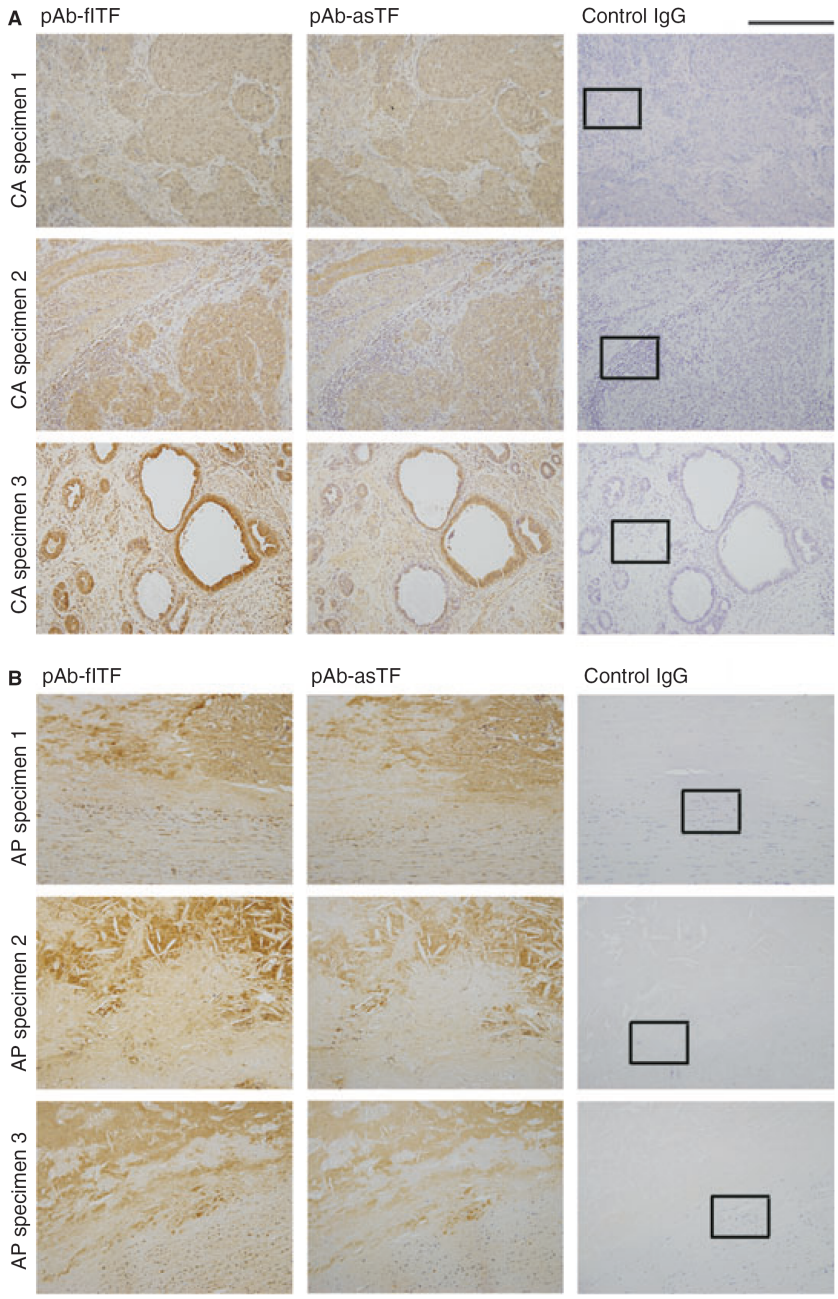

Fig. 1. Representative images, localization of fITF and asTF in paraffin-embedded specimens of cervical cancer tissue (A) and lipid-rich aortic plaques (B). CA, cervical adenocarcinoma; AP, aortic plaque. Final dilution for all primary antibodies, 2.0 µg/mL^{-1}; original magnification, 20x; scale bar, 250 µm. In black boxes: the regions analyzed by immunofluorescence as shown in Fig.3.

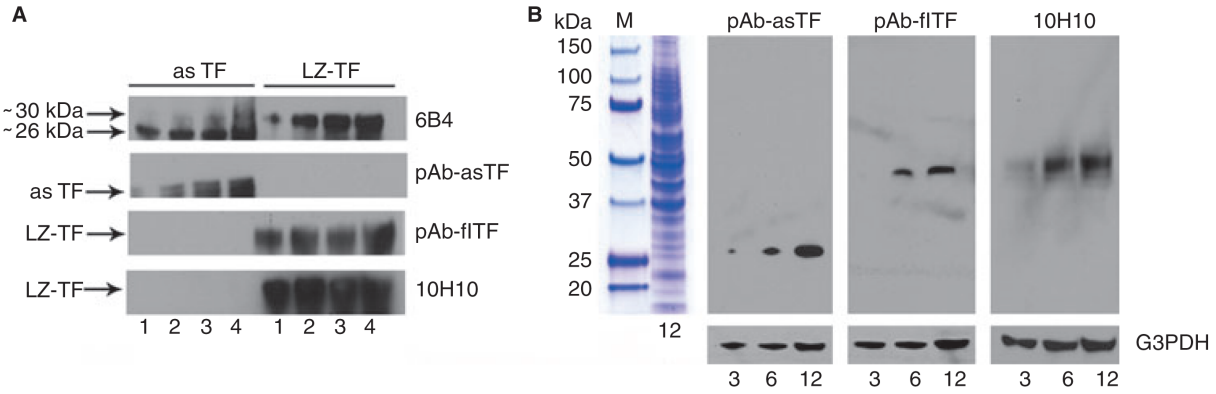

Fig. 2. Characterization of the anti-human TF antibodies used in the study. (A) Reactivity of the four antibodies with recombinant asTF and LZ-TF; the indicated amounts of protein are in ng. **(B)** Specificity of the isoform-specific anti-TF antibodies: the indicated amounts of total protein (lysatesof cervical adenocarcinoma) are in µg; M, molecular weight marker with the adjacent lane showing the lysate stained with Coomassie; blots were stripped and re-probed with anti-G3PDH antibody.

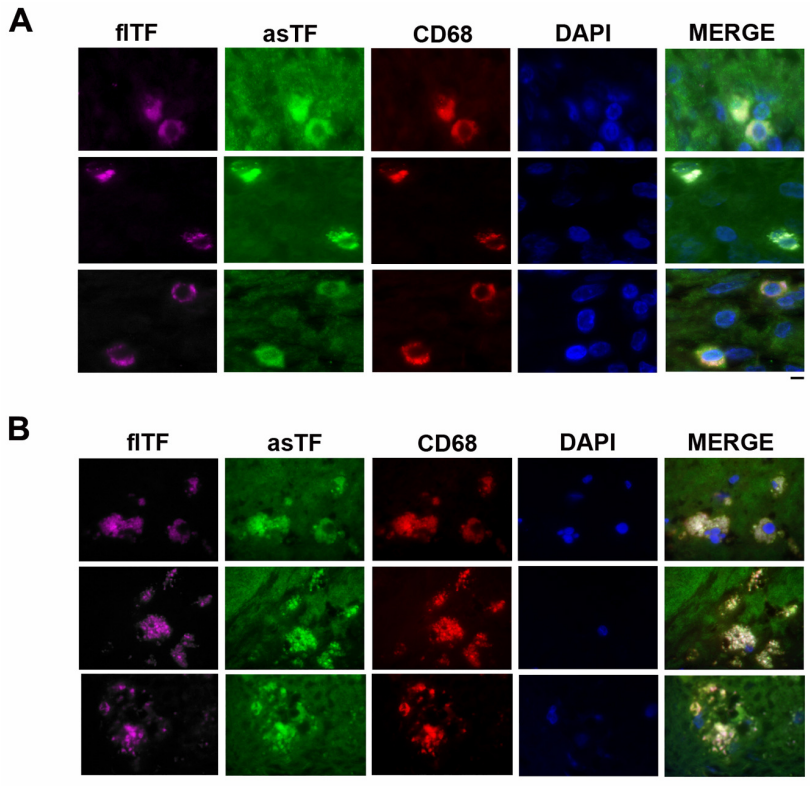

Fig. 3. Representative images, co-localization of CD68^{+} cells (red), flTF (purple) and asTF (green) in cervical cancer tissue specimens (A) and lipid-richaortic plaques (B). Final dilution for all primary antibodies, 2.0 µg mL^{-1}; original magnification, 100x; scale bar, 2 µm.

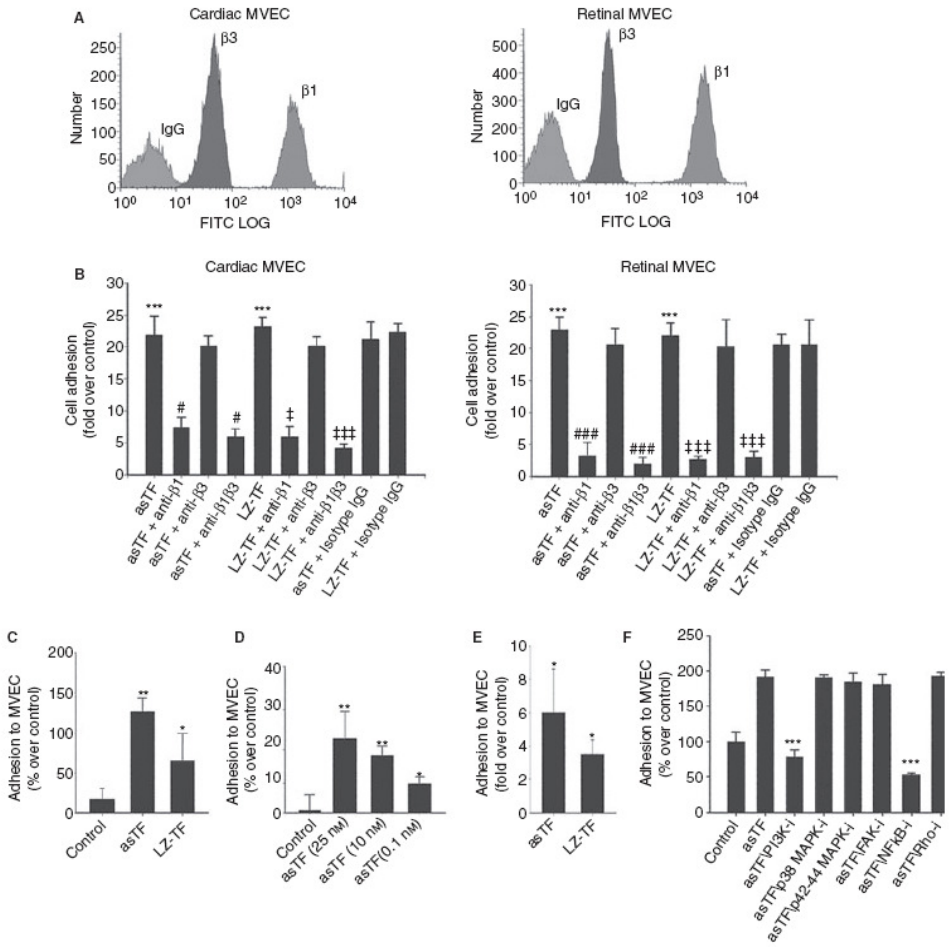

Fig. 4. LZ-TF and asTF ligate β1 integrins on human MVEC and promote MVEC-monocyte interactions. (A). Flow cytometry, relative levels of β1/β3integrins on the surfaces of cardiac and retinal MVEC. **(B)** MVEC adhesion to LZ-TF/asTF (n ≥3). Values are mean ± SD; *** $P < 0.001$ comparedwith BSA; and ###, $P < 0.05$ and $P < 0.001$, respectively, compared with asTF; ‡ and ‡‡‡, $P < 0.05$ and $P < 0.001$, respectively, compared with LZ-TF. **(C)** LZ-TF and asTF promote MVEC-PBMC interactions in the orbital shear assay. **(D)** Dose-response experiments, asTF in the orbital shear assayemploying PBMCs. **(E)** LZ-TF and asTF promote MVEC-PBMC interactions in the laminar flow assay. **(F)** Effects of kinase inhibition on asTF-triggered MVEC-monocyte interactions under orbital shear; MVEC were preincubated with PI3 kinase inhibitor LY294002 (10 μM), p38 MAPK inhibitor SB203580 (10 μM), p42/p44 MAPK inhibitor PD98059 (20 μM), FAKII inhibitor (10 μM), NFκB inhibitor BMS345541 (10 μM), and Rho kinase inhibitor (10 μM). * $P < 0.01$, ** $P < 0.001$, *** $P < 0.0001$. n ≥ 3 for each assay, the values are mean ± SD. #, $P < 0.05$ compared with asTF. ‡ and ‡‡, $P < 0.05$ and $P < 0.01$, respectively, compared with LZ-TF.

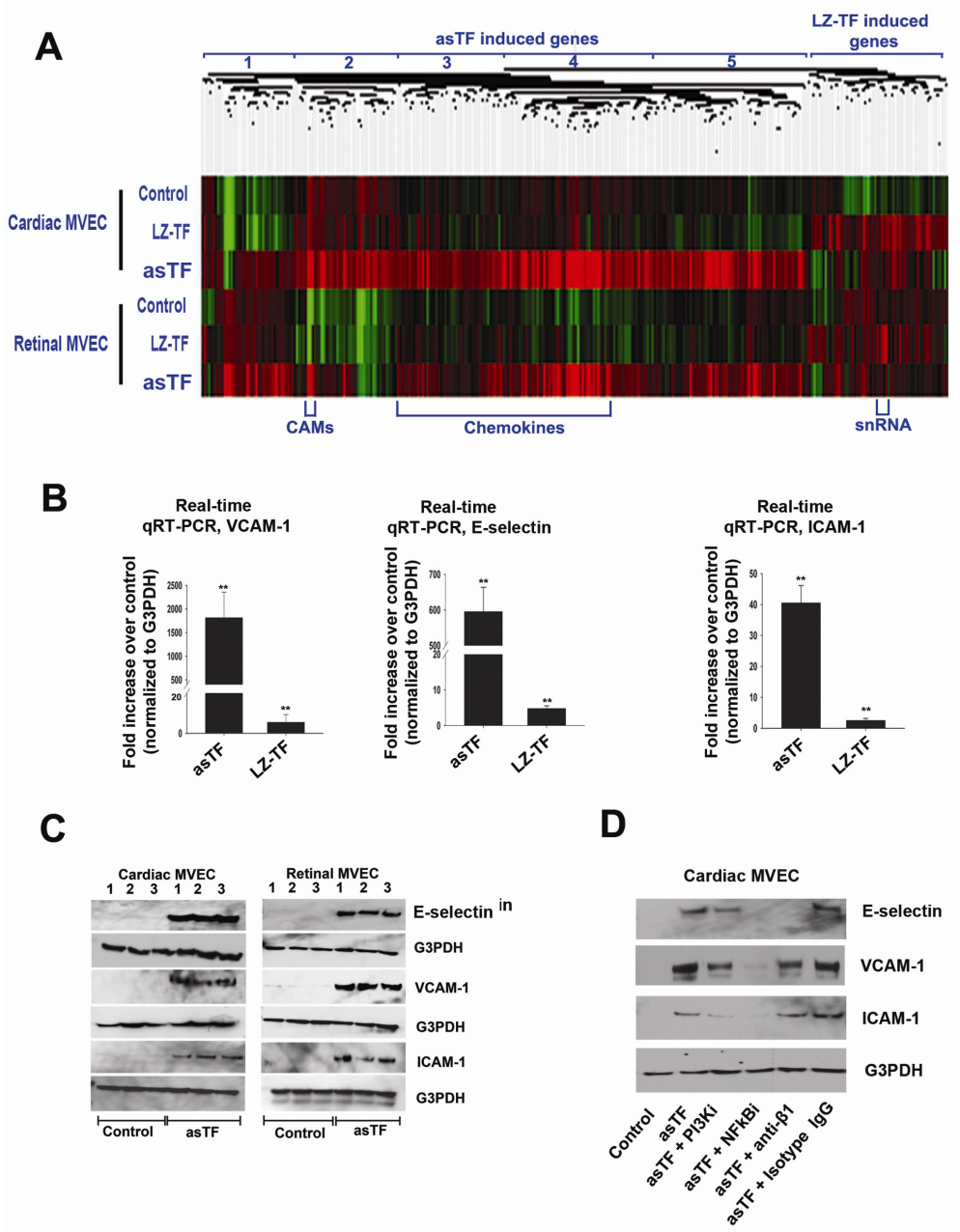

Fig. 5. (A) Heat map, asTF- and LZ-TF-stimulated cardiac and retinal MVEC; see text for details on gene clusters 1–5. (B) Real-time quantitative RT-PCR for VCAM-1, ICAM-1 and E-selectin (n = 3). **(C)** Western blotting for E-selectin, VCAM-1 and ICAM-1 (samples from three independent experiments are shown). **(D)** Effects of pharmacologic inhibitors and anti-β1 antibody on asTF-triggered expression of CAMs in MVEC; blots were stripped and re-probed with anti-G3PDH antibody.

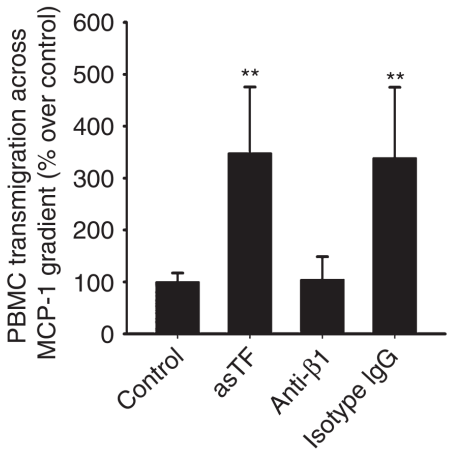

Fig. 6. Transwell assay under MCP-1 gradient (50 µg/L). PBMCs on the abluminal surface of the inserts chamber were stained with DAPI and counted using Image J (n=3, mean ± SD, **p<0.001).

Category type	Category name	*P*-value
Biological process	Cell adhesion	5.58E-03
Biological process	Locomotion	1.04E-04
Biological process	Leukocyte migration	8.79E-04
Molecular function	Receptor binding	1.50E-04
Molecular function	Cytokine activity	2.56E-04
Pathway	Cytokine-receptor interaction	8.65E-06
Pathway	TNF receptor signaling	6.13E-04
Co-expression	Genes upregulated by TNF	8.57E-16
Genes with transcription factor binding site	GATTGGY (NFkB)	1.79E-04
Genes with transcription factor binding site	TTGCWCAAY (CEBP)	9.76E-04

Table 1. Summary of the pathways and genes maximally activated by asTF in cardiac and retinal MVEC

Supplementary material

Antibodies, chemicals, cell culture supplies- Anti-CD68 (cat. # IMG80071) and anti-CD34 (cat. # IMG80073) monoclonal antibodies were from Imgenex. Anti-β3 integrin (cat. # MAB197Z), anti-β1 integrin (cat. # MAB17781), anti E-selectin (cat. # AF724), and anti-VCAM-1 (cat. # AF809) monoclonal antibodies were from R&D Systems. Anti-ICAM-1 monoclonal rabbit antibody was from Epitomics (cat. # 1929-1). Calcein-AM was obtained from BD Biosciences (cat. # 354216). Cell culture inserts were from Millipore. Kinase inhibitors LY294002 (cat. # 44024), SB20380 (cat. # 559398), PD98059 (cat. # 98059), FAK inhibitor II (cat. # 324878), and Rho kinase inhibitor (cat. # 55552) were obtained from Calbiochem. NFκB inhibitor BMS-345541 (cat. # B9935) was obtained from Sigma-Aldrich. Anti-human TF monoclonal antibody 6B4 was described previously (van den Berg et al,

PNAS '09 and references therein). Anti-human flTF antibody 10H10 (mouse monoclonal) was previously described (van den Berg et al, PNAS '09 and references therein); custom anti-human flTF and anti-human asTF rabbit polyclonal antibodies were previously described (Tardos et al, JTH '08). Isotype control IgG (ChromPure grade) were obtained from Jackson ImmunoResearch. T75 Cell culture flasks and other cell culture disposables were purchased from Greiner Bio-One (Alphen a/d Rijn, the Netherlands).

Immunofluorescence studies- Paraffin embedded specimens of human cervical adenocarcinoma and lipid-rich aortic plaques were used to study the co-localization of flTF, asTF, and CD68. Tissue sections were deparaffinized, blocked, and incubated with specific anti-flTF antibody 10H10 and specific polyclonal anti-asTF antibody for 3 hrs at RT. The slides were then washed and incubated with Alexa fluor-488 labeled goat anti-rabbit antibody and Alexa fluor-633 labeled goat anti-mouse antibody (Invitrogen) for 1hr at RT. The slides were then extensively washed and incubated with phycoerythrin-labeled anti-CD68 antibody for 1hr at RT. The slides were further washed and mounted with vectashield containing DAPI (Vector Labs). Images were captured and pseudo-colored when needed to discriminate between asTF (green), flTF (purple), and CD68 (red).

RT-PCR- Total RNA was isolated using RNAeasy Kit (Qiagen), reverse transcribed using Transcriptor (Roche Diagnostics), and PCR-amplified using FastStart Taq polymerase (Roche Diagnostics). Amplicons were separated on 2% agarose and visualized using ethidium bromide. Real time qRT-PCR for E-selectin, VCAM-1, and ICAM-1 was performed using TaqMan probes from the Universal Probe Library, Roche Diagnostics.

Western blotting- MVEC were grown to confluence in 6-well plates, treated with asTF or vehicle control for 4 hrs, and then lysed directly in Laemmli sample buffer. Lysates were loaded on 10% SDS-PAGE gels and, following electrophoresis, transferred to PVDF membranes (Roche Diagnostics). Membranes were blocked with 2% dry skim milk in Tris-buffered saline/Tween-20 (TBST) overnight at 4ºC, incubated with the primary antibodies against ICAM-1, VCAM-1, or E-selectin for 3 hrs at room temperature, washed in TBST, and then incubated with the corresponding HRP-conjugated secondary antibodies (Invitrogen) for 1 hr room temperature. Chemiluminescence was obtained using LumiLight (Roche Diagnostics). For the characterization of anti-human TF antibodies' reactivity and specificity, recombinant TF protein variants and cervical cancer lysates, respectively, were probed with 6B4, 10H10, and custom polyclonal antibodies selectively recognizing flTF and asTF.

Removal of N-His tag from recombinant asTF- Recombinant N-His tagged asTF was treated with 1U of rEnterokinase (rEK, Novagen) for 16 hrs at room temperature, following which

rEK was removed using enterokinase cleavage-capture kit (Novagen). The asTF purity and MW were confirmed on 10% PAGE stained with Coomasie brilliant blue. Prior to experiments, asTF concentration was measured using Bradford microassay.

Supplementary Figures

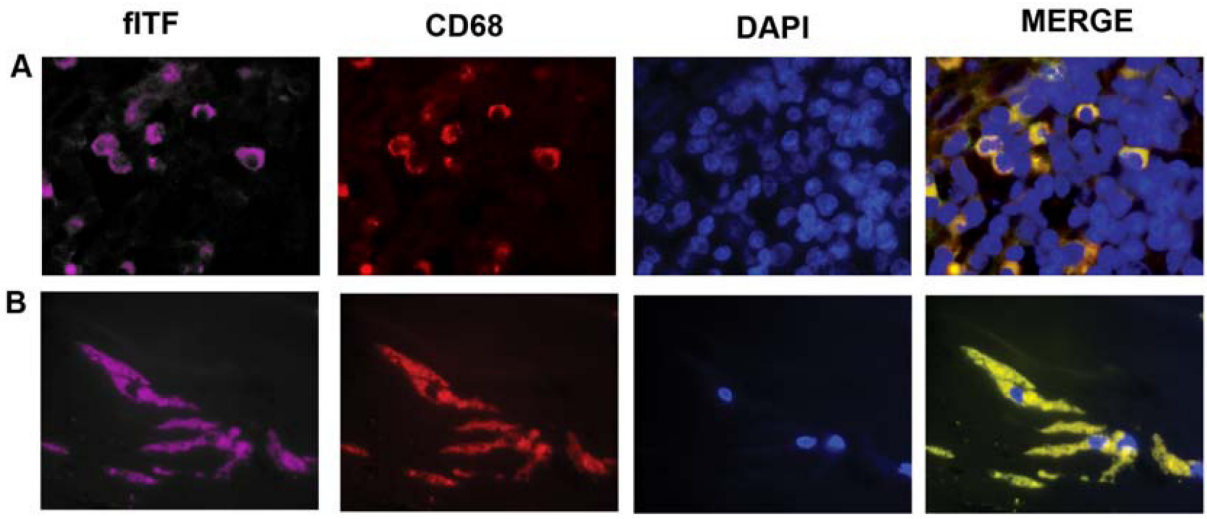

Fig. S1. Representative images, co-localization of flTF and CD68 in paraffin-embedded specimens of cervical cancers (A) and aortic plaques (B) assessed using flTF-specific rabbit polyclonal antibody and anti-CD68 monoclonal antibody. Following incubation with the primary antibodies, slides were washed, incubated with fluorophore-labeled corresponding secondary antibodies, and mounted with vectashield containing DAPI (Vector Labs). Visualization was performed in a Nikon-Photostat fluorescent microscope; images were captured using a CCD camera.

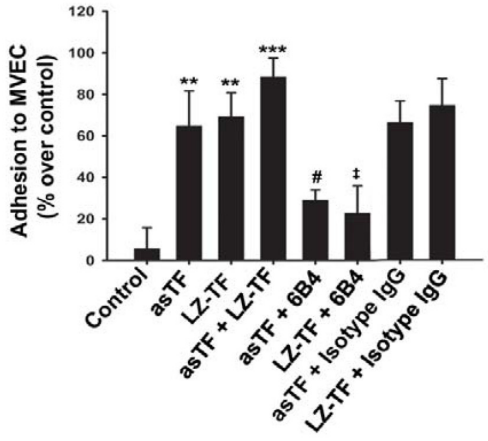

Fig. S2. LZ-TF and asTF promote MVEC-monocyte interactions via integrin ligation. Blockade of integrin binding by anti-TF antibody 6B4 inhibits MVEC-THP-1 interactions. n=3 for each assay, the values are mean ± SD. *, **, *** $p<0.05$, $p<0.01$ and $p<0.001$, respectively, compared to control. # $p<0.05$ compared to asTF. ‡ and ‡‡ $p<0.05$ and $p<0.01$, respectively, compared to LZ-TF.

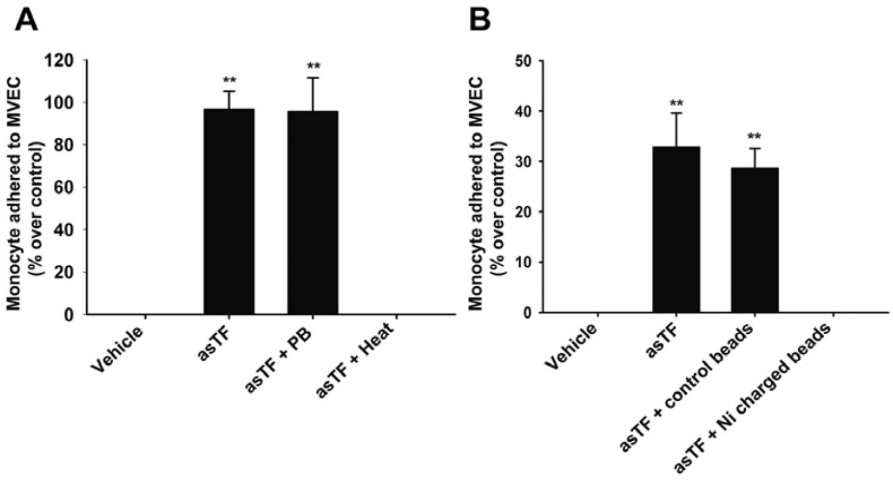

Fig. S3. (A) MVEC were treated with recombinant asTF, or pre-treated with Polymyxin B ("PB," 50 µg/ml) prior to the addition of recombinant asTF; in a separate sample, the medium containing recombinant asTF was heated and added to MVEC; monocyte-MVEC interactions were assessed using orbital shear assay. **(B)** Ni-charged and uncharged (control) beads were added to the medium containing recombinant asTF and placed on a rocker platform for 1 hr at room temperature; beads were removed by centrifugation and the medium was then added to MVEC. Monocyte-MVEC interactions were assessed using orbital shear assay. **p< 0.001.

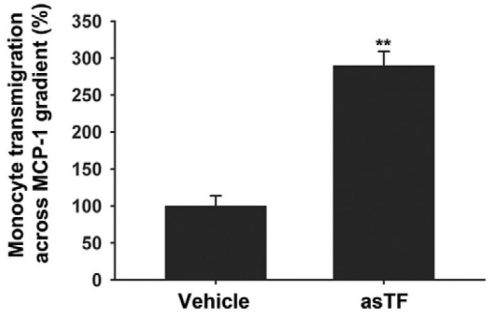

Fig. S4. Transwell assay under MCP-1 gradient (50 µg/L). THP-1 cells on the abluminal surface of the inserts chamber were stained with DAPI and counted using Image J (n=3, mean ± SD, **p<0.001).

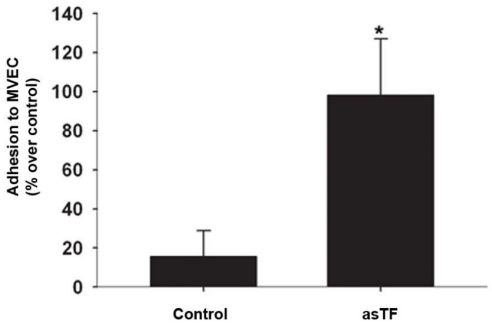

Fig. S5. Increased MVEC-monocyte adhesion elicited by recombinant asTF lacking the N-terminal His-tag, orbital shear assay. * p< 0.01

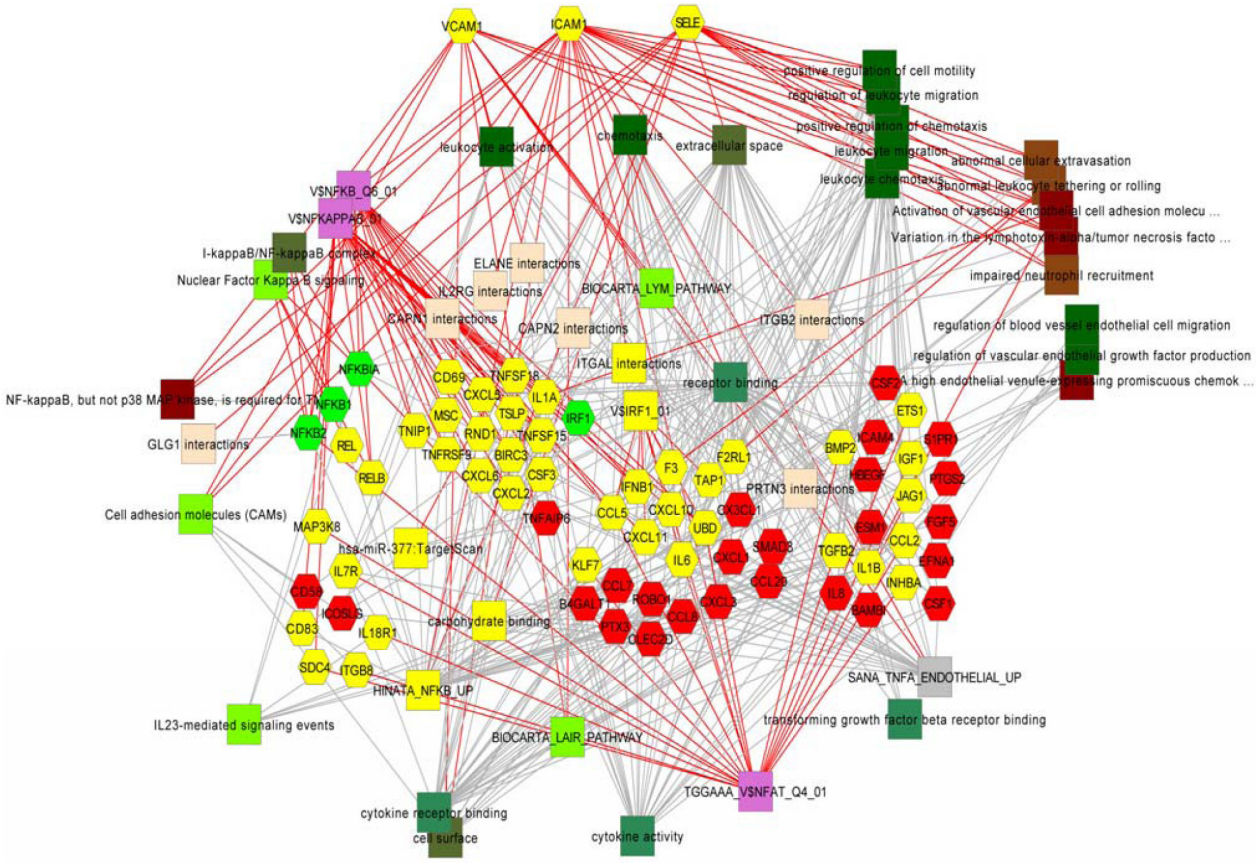

Fig. S6. Schematic representation of the interactions between the major pathways upregulated in MVEC stimulated with asTF. Yellow hexagons: primary NFkB targets; red hexagons: targets of the NFkB-upregulated genes. Grouped color-coded squares: the affected physiological and pathophysiological pathways (green and brown, respectively).

Supplementary table. Top 30% of the genes upregulated ~1.5 fold in cardiac and retinal MVEC in response to asTF stimulation.

S.no	Gene name (HUGO)	Gene Description	Cardiac MVEC	Retinal MVEC
			Fold over control	Fold over control
1	CCL20	chemokine (C-C motif) ligand 20	30.4	14.8
2	TNFAIP6	tumor necrosis factor, alpha-induced protein 6	17.8	5.6
3	TNIP3	TNFAIP3 interacting protein 3	17.8	14.0
4	CXCL3	chemokine (C-X-C motif) ligand 3	16.3	7.8
5	TNFAIP3	tumor necrosis factor, alpha-induced protein 3	11.7	5.3
6	IL18R1	interleukin 18 receptor 1	10.3	4.6
7	BIRC3	baculoviral IAP repeat-containing 3	9.9	13.2
8	IL1B	interleukin 1, beta	9.8	1.5
9	HIVEP2	human immunodeficiency virus type I enhancer binding protein 2	9.5	3.9
10	IL6	Interleukin 6 (interferon, beta 2)	9.3	7.3
11	CXCL2	chemokine (C-X-C motif) ligand 2	9.0	17.5
12	IL8	interleukin 8	8.9	12.2
13	SELE	selectin E (endothelial adhesion molecule 1)	8.1	108.4
14	SLC7A2	solute carrier family 7 (cationic amino acid transporter, y+ system), member 2	7.2	3.4
15	RND1	Rho family GTPase 1	6.1	3.6
16	MSC	musculin (activated B-cell factor-1)	6.1	1.7
17	CXCL1	chemokine (C-X-C motif) ligand 1 (melanoma growth stimulating activity, alpha)	5.9	7.4
18	VCAM1	vascular cell adhesion molecule 1	5.4	40.5
19	CCL5	chemokine (C-C motif) ligand 5	5.3	2.2
20	IL1A	interleukin 1, alpha	5.1	3.4
21	CLEC2D	C-type lectin domain family 2, member D	4.8	3.6
22	NFKBIZ	nuclear factor of kappa light polypeptide gene enhancer in B-cells inhibitor, zeta	4.7	4.0

S.no	Gene name (HUGO)	Gene Description	Cardiac MVEC	Retinal MVEC
			Fold over control	Fold over control
23	ICAM1	intercellular adhesion molecule 1 (CD54), human rhinovirus receptor	4.6	8.7
24	TNFAIP2	tumor necrosis factor, alpha-induced protein 2	4.5	2.4
25	CSF2	colony stimulating factor 2 (granulocyte-macrophage)	4.4	2.8
26	ELOVL7	ELOVL family member 7, elongation of long chain fatty acids (yeast)	4.3	1.8
27	SOD2	superoxide dismutase 2, mitochondrial	4.2	4.4
28	IFIH1	interferon induced with helicase C domain 1	4.1	4.7
29	EFNA1	ephrin-A1	4.1	2.4
30	RIPK2	receptor-interacting serine-threonine kinase 2	4.1	3.4
31	TNFRSF9	tumor necrosis factor receptor superfamily, member 9	4.0	2.4
32	IRF1	interferon regulatory factor 1	3.9	1.5
33	SLC41A2	solute carrier family 41, member 2	3.9	2.0
34	UBD	ubiquitin D	3.9	2.2
35	CD69	CD69 molecule	3.8	6.0
36	F3	coagulation factor III (thromboplastin, tissue factor)	3.8	2.0
37	CXCR7	chemokine (C-X-C motif) receptor 7	3.6	1.9
38	PTGS2	prostaglandin-endoperoxide synthase 2 (prostaglandin G/H synthase and cyclooxygenase)	3.6	2.9
39	TIFA	TRAF-interacting protein with a forkhead-associated domain	3.6	3.6
40	UBD	ubiquitin D	3.5	2.1
41	ZC3H12C	zinc finger CCCH-type containing 12C	3.4	2.6
42	IL7R	Interleukin 7 receptor	3.4	2.4
43	TRAF1	TNF receptor-associated factor 1	3.3	1.8
44	FGF5	fibroblast growth factor 5	3.1	2.5
45	TNFAIP8	tumor necrosis factor, alpha-induced protein 8	3.1	1.8

S.no	Gene name (HUGO)	Gene Description	Cardiac MVEC	Retinal MVEC
			Fold over control	Fold over control
46	PDE5A	phosphodiesterase 5A, cGMP-specific	3.0	1.9
47	NFKB1	nuclear factor of kappa light polypeptide gene enhancer in B-cells 1 (p105)	3.0	2.6
48	BCL2A1	BCL2-related protein A1	3.0	2.9
49	IRAK2	interleukin-1 receptor-associated kinase 2	2.9	2.0
50	NFKBIA	nuclear factor of kappa light polypeptide gene enhancer in B-cells inhibitor, alpha	2.9	3.6
51	CXCL6	chemokine (C-X-C motif) ligand 6 (granulocyte chemotactic protein 2)	2.8	2.5
52	MAP3K8	mitogen-activated protein kinase kinase kinase 8	2.8	2.1
53	IFIT3	interferon-induced protein with tetratricopeptide repeats 3	2.6	2.2
54	CNKSR3	CNKSR family member 3	2.5	2.2
55	ICOSLG	inducible T-cell co-stimulator ligand	2.5	1.6
56	SDC4	syndecan 4	2.5	2.7
57	CYLD	cylindromatosis (turban tumor syndrome)	2.4	2.1
58	WTAP	Wilms tumor 1 associated protein	2.4	1.5
59	CD83	CD83 molecule	2.3	1.6
60	GBP4	guanylate binding protein 4	2.3	2.3
61	SERPINB2	serpin peptidase inhibitor, clade B (ovalbumin), member 2	2.3	1.7
62	CSF1	colony stimulating factor 1 (macrophage)	2.3	1.6
63	OSGIN2	oxidative stress induced growth inhibitor family member 2	2.3	1.5
64	RELB	v-rel reticuloendotheliosis viral oncogene homolog B, nuclear factor of kappa light polypeptide gene enhancer in B-cells 3 (avian)	2.2	2.0
65	CLDN1	claudin 1	2.2	1.9
66	CSF3	colony stimulating factor 3 (granulocyte)	2.2	1.7
67	MMP10	matrix metallopeptidase 10 (stromelysin 2)	2.2	2.2

S.no	Gene name (HUGO)	Gene Description	Cardiac MVEC	Retinal MVEC
			Fold over control	Fold over control
68	IFIT2	interferon-induced protein with tetratricopeptide repeats 2	2.1	2.6
69	DRAM	damage-regulated autophagy modulator	2.0	1.5
70	CCL2	chemokine (C-C motif) ligand 2	2.0	6.7
71	CTSS	cathepsin S	2.0	1.8